Numerical simulation of nonlinear wave propagation over a bar

S. Beji[1], J.A. Battjes

Delft University of Technology, Department of Civil Engineering, Stevinweg 1, P.O. Box 5048, 2600 GA Delft, Netherlands

Abstract

Numerical computations based on a one-dimensional time domain Boussinesq model with improved dispersion characteristics are carried out to model relatively long, unidirectional waves propagating over a submerged obstacle. Comparisons for non-breaking waves show good agreement between the numerical results and measurements obtained from experiments in a wave flume with a submerged trapezoidal bar. The observed phenomena of bound harmonics generation in the shoaling region (upslope) and their release, or wave decomposition, in the deepening part of the flume (downslope) are well predicted by the numerical model both for regular and random waves. The inclusion of the effects of wave breaking is briefly discussed.

1. Introduction

Harmonic generation in an initially narrow-banded spectrum of a wave field propagating over a submerged obstacle has long been known both empirically and theoretically.

Johnson et al. (1951) noted that over natural reefs the energy was transmitted as a multiple crest system. Jolas (1960) carried out experiments with a submerged shelf of rectangular section and observed harmonics of a simple incident wave on the transmission side when the water depth above the bar was shallow enough. Based on field measurements in nearshore regions with bar–trough type bathymetries, Byrne (1969), Dingemans (1989) and Young (1989) reported the same type of findings. Recently Rey et al. (1992) reported detailed laboratory observations in the same vein.

On the other hand, the phenomenon of harmonic generation has been explained theoret-

---

[1]Former post-doctorate fellow. Present address: Naval Architecture and Ocean Engineering Faculty, Istanbul Technical University, Turkey.

ically, on the basis of nonlinear equations for shallow-water waves, usually after Boussinesq or Korteweg and de Vries. These theories were re-established by Friedrichs (1948), Ursell (1953) and Mei and Le Méhauté (1966) on firm and rigorous bases. Peregrine (1967) presented a formulation, basically of Boussinesq-type, for nonlinear dispersive waves on a mildly sloping beach, which became a prototype for many studies of the same kind.

Beginning from the 1970's Abbott and co-workers have developed numerical schemes for solving one- and two-dimensional wave propagation problems via Boussinesq models (Abbott et al., 1973; Abbott, 1974; Abbott et al., 1978, 1984). Following a slightly different approach, Schaper and Zielke (1984) developed an alternative scheme, including corrections to truncation errors, which was later enhanced by Prüser et al. (1986) and applied to various cases including irregular waves.

In recent years, several improvements have been developed in the Boussinesq equations. Witting (1984) introduced a formulation with improved dispersion characteristics. Madsen et al. (1991a) utilized Witting's result to derive a new set of Boussinesq equations for horizontal bottom, containing additional third-order derivatives as compared to the conventional equations. This leads to improved dispersion for the higher-frequency components, effectively out to deep-water waves. Their technique was applied by Battjes and Beji (1991) and by Madsen and Sørensen (1992) to Boussinesq equations for mildly sloping bottoms.

The formulations referred to above are in the time domain. Parallel to these, frequency-domain formulations have been developed, leading to coupled evolution equations for slowly varying amplitudes and phases of harmonic components, similar to the work by Bryant (1973) for Stokes waves. Reference is made to Freilich and Guza (1984) and Kirby (1990) for frequency-domain versions of conventional equations and to Madsen et al. (1991b), Madsen and Sørensen (1993) and Mase and Kirby (1992) for extended equations, with improved linear shoaling and dispersion characteristics.

In this paper we present the development and results of numerical computations based on a Boussinesq model for sloping bottoms with improved dispersion characteristics. We consider an isolated submerged obstacle, which poses a challenging case due to the phenomenon of wave decomposition taking place in the deepening region behind the obstacle. Release of bound harmonics past the obstacle, or wave decomposition, gives rise to rapidly varying wave forms, which can be simulated accurately only by a sufficiently nonlinear model with good dispersion characteristics.

The scheme employed here is essentially based on the formulation introduced by Peregrine (1967) but it differs in three aspects; namely, additional terms for improving the dispersion characteristics obtained as in Madsen et al. (1991a), the discretization of the continuity equation, and the treatment of the advective term. The development thus far is restricted to non-breaking waves. Work on inclusion of the effects of breaking is still in progress and will be reported separately; here we only mention it.

The following section recapitulates the original and improved governing equations. Details of the numerical scheme are given in section 3. Comparisons of numerical computations with results of laboratory measurements are presented in section 4. The inclusion of dissipation by breaking is briefly discussed in section 5.

2. Governing equations

2.1. Original equations

Equations of motion describing relatively long, small amplitude waves propagating in water of varying depth are given by Peregrine (1967):

$$u_t + (u \cdot \nabla)u + g\nabla\zeta = \frac{1}{2}h\frac{\partial}{\partial t}\nabla[\nabla\cdot(hu)] - \frac{1}{6}h^2\frac{\partial}{\partial t}\nabla(\nabla\cdot u) \tag{1}$$

$$\frac{\partial\zeta}{\partial t} + \nabla\cdot[(h+\zeta)u] = 0 \tag{2}$$

where ζ is the surface displacement, u is the depth-averaged horizontal velocity vector, and h is the still water depth. For constant depth the above equations reduce to the well-known original Boussinesq equations.

If the spatial variations of bottom geometry are considered mild and second — and higher — order space derivatives of the sea bed elevation are neglected, the above equations, for one-dimensional propagation, read:

$$u_t + uu_x + g\zeta x = \frac{1}{3}h^2 u_{xxt} + hh_x u_{xt} \tag{3}$$

$$\zeta_t + [(h+\zeta)u]_x = 0 \tag{4}$$

where the subscripts denote partial differentiation with respect to the indicated indices and u is the depth-averaged velocity component in the x-direction.

In general, Eqs. (1) and (2) describe waves with small but not infinitesimal amplitude, relatively long but not so long that the effects of depth attenuation on the pressure field are ignored completely. In other words, the equations represent weak nonlinearity and dispersion. A lucid derivation of these equations for constant depth in terms of a nonlinearity parameter and a dispersion parameter can be found in Mei (1989).

2.2. Boussinesq equations with improved dispersion characteristics

In recent years the original Boussinesq equations have been successfully used to model wave phenomena in the near-shore zone, such as shoaling, refraction, diffraction, harmonic generation, etc. (see references cited in the Introduction). However, their poor dispersion characteristics in depths greater than about 20% of the wave length have been a major obstacle particularly in dealing with waves approaching from offshore. Several attempts have been made to improve the dispersion characteristics of the Boussinesq-type equations so that their excellent properties in the nearshore zone could be extended to deeper water.

Witting (1984) expressed the vertically averaged velocity and the surface velocity in terms of a pseudo velocity expanded in Taylor series with coefficients different from the usual Taylor coefficients. These coefficients in turn were determined by matching with the Padé expansion of the linear theory phase celerity.

Inspired by Witting's formulation, Madsen et al. (1991a) gave a formulation for hori-

zontal bottom in which they added third-order derivative terms with an adjustable propor-
tionality factor (calibration factor) b. This was shown to give a very effective improvement
of the linear dispersion characteristics. Battjes and Beji (1991) applied the technique of
Madsen et al. (1991a) to Peregrine's form of the Boussinesq equations for mildly sloping
bottoms (Eq. 1 given above). For the one-dimensional case, as considered here, the result
is

$$u_t + uu_x + g\zeta_x = \frac{1}{3}h^2 u_{xxt} + hh_x u_{xt} + bh^2(u_{xxt} + g\zeta_{xxx}) \tag{5}$$

$$\zeta_t + [(h+\zeta)u]_x = 0 \tag{6}$$

This set of equations is used in the following. The set used by Madsen et al. (1991a), as
well as the extended version thereof by Madsen and Sørensen (1992), which allows for
small bottom slopes, is formulated in conservative form for the vertically integrated momen-
tum rather than in acceleration form for the vertically averaged velocity (u), which we have
preferred because it results in a simpler momentum equation. This difference in formulation
causes a small discrepancy between the bottom-slope terms in the momentum equation of
Madsen and Sørensen (1992) and Eq. (5), respectively. However, this is of the order of
magnitude of terms already neglected in the derivations.

The factor b in Eq. (5) is not determined from first principles. It is free to take on any
value that minimizes the overall phase celerity errors. Madsen et al. (1991a) suggest the
value $b = 1/21$ as the one that leads to celerity errors less than 3% for depth-to-wavelength
ratios up to 0.75. In our computations however the best agreement with the measurements
was obtained for $b = 1/15$, which corresponds to a simpler form of Witting's original
formulation. In a later publication, Madsen et al. (1991b) have also favored $b = 1/15$ rather
than $b = 1/21$.

3. Discretisation

3.1. Finite differences approximations

It appears that the first numerical solutions of Boussinesq-type equations in the nearshore
zone may be credited to Peregrine (1967), who also gave a formal derivation of these
equations for a mildly sloping bottom and estimated the amplitude of waves reflected from
the slope. Actually, a year earlier, Mei and Le Méhauté (1966) had derived the same type
of equations in a different manner and outlined a numerical scheme based essentially on
the method of characteristics but they did not include any computations.

In discretizing the momentum equation we shall basically follow Peregrine (1967) but
the discretization of the continuity equation will be different because we base it on the
conservation form, Eq. (6), rather than expanding the volume flux term. First, an explicit
formulation of the continuity equation is used to obtain a first estimate of the surface
displacements at the new time level ($j+1$):

$$\frac{\zeta_{i,j+1} - \zeta_{i,j}}{\Delta t} + \frac{[(h+\zeta)u]_{i+1,j} - [(h+\zeta)u]_{i-1,j}}{2\Delta x} = 0 \tag{7}$$

where the indices i and j stand respectively for the integers multiplying the increments in space and time.

This first estimate of the surface displacements is used in an implicit discretization of the momentum equation, Eq. (5) with $b = 1/15$, to compute the velocity at the new time level $(j + 1)$:

$$\frac{u_{i,j+1} - u_{i,j}}{\Delta t} + u_{i,j+1/2} \frac{u_{i+1,j+1} - u_{i-1,j+1} + u_{i+1,j} - u_{i-1,j}}{4\Delta x}$$

$$+ g \frac{\zeta_{i+1,j+1} - \zeta_{i-1,j+1} + \zeta_{i+1,j} - \zeta_{i-1,j}}{4\Delta x}$$

$$= \frac{2}{5} h_i^2 \frac{u_{i+1,j+1} - 2u_{i,j+1} + u_{i-1,j+1} - u_{i+1,j} + 2u_{i,j} - u_{i-1,j}}{\Delta x^2 \Delta t}$$

$$+ h_i \frac{h_{i+1} - h_{i-1}}{2\Delta x} \frac{u_{i+1,j+1} - u_{i-1,j+1} - u_{i+1,j} + u_{i-1,j}}{2\Delta x \Delta t}$$

$$+ \frac{1}{15} gh_i^2 \frac{\zeta_{i+2,j+1} - 2\zeta_{i+1,j+1} + 2\zeta_{i-1,j+1}}{4\Delta x^3}$$

$$+ \frac{1}{15} gh_i^2 \frac{-\zeta_{i-2,j+1} + \zeta_{i+2,j} - 2\zeta_{i+1,j} + 2\zeta_{i-1,j} - \zeta_{i-2,j}}{4\Delta x^3} \tag{8}$$

Note that central differences formulations are used both for time and space derivatives, which are computed at $(i, j + 1/2)$. The above formulation is suitable for application of the double-sweep algorithm which is the most efficient way of solving a tri-diagonal matrix system as long as the diagonal elements are dominant.

Finally, the following discretization of the continuity equation is applied with the use of the new time level velocity field obtained from Eq. (8) and the provisional surface elevation from Eq. (7) in the nonlinear terms:

$$\frac{\zeta_{i,j+1} - \zeta_{i,j}}{\Delta t}$$
$$+ \frac{[(h + \zeta)u]_{i+1,j+1} - [(h + \zeta)u]_{i-1,j+1} + [(h + \zeta)u]_{i+1,j} - [(h + \zeta)u]_{i-1,j}}{4\Delta x} = 0 \tag{9}$$

From this equation, improved estimates are obtained of the surface elevations at the new time level. Iteration between Eqs. (8) and (9) could have been carried out but was found to be unnecessary.

In Eq. (8), the factor $u_{i,j+1/2}$ in the advective acceleration term denotes the value of depth-averaged horizontal velocity at time $t + \frac{1}{2}\Delta t$. It arises because all the derivatives are centered. In the original formulation, Peregrine (1967) uses the old time level value, $u_{i,j}$ as an approximation. Our computational tests with steep solitary waves however showed that this causes a gradual but consistent decay in wave height as time progresses. It was therefore necessary to estimate $u_{i,j+1/2}$.

To do this, we begin with the following Taylor series expansion truncated at the first order:

$$u_{i,j} = u_{i,j+1/2} - \frac{\Delta t}{2} \frac{\partial u}{\partial t}\bigg|_{i,j+1/2} + \ldots \tag{10}$$

In order to estimate u_t at time $t + \frac{1}{2}\Delta t$, we first approximate u_t by employing the momentum equation for the shallow water approximation, $u_t \approx -uu_x - g\zeta_x$. The term u_x can be computed only at time t. We can however replace it with the time derivative of the surface displacement by employing the linearized continuity equation, $u_x = -\zeta_t/h$. After solving Eq. (10) for $u_{i,j+1/2}$ and substituting all the replacement terms we obtain:

$$u_{i,j+1/2} \approx u_{i,j} + \frac{\Delta t}{2}\left[\frac{1}{h}\frac{\partial \zeta}{\partial t}u - g\frac{\partial \zeta}{\partial x}\right]_{i,j+1/2} \tag{11}$$

Except for the term $u_{i,j+1/2}$, all the quantities on the right are available because at this stage of our routine we have solved the continuity equation explicitly and obtained the surface displacement (provisional value) at the new time level. The factor $u_{i,j+1/2}$ on the right can be handled in three different ways. The simplest is to replace it with $u_{i,j}$, the value at time t. A better way is to take it to the left side of the equation, combine it with the other $u_{i,j+1/2}$ term there and then solve for $u_{i,j+1/2}$. The third approach is to expand it in a Taylor series as in Eq. (10), and then to replace u_t with $-g\zeta_x$. In our computations we have employed the last approach.

Estimation of $u_{i,j+1/2}$ as described above did not completely cure the wave height decay observed in numerical simulations of very steep solitary waves; however it did provide visible improvements and therefore was included in the numerical scheme.

3.2. Initial and boundary conditions

The initial condition used in all our computations is the unperturbed state; that is, at time $t = 0$ both the surface displacements and the velocities are set to zero throughout the computational domain.

The boundary conditions are handled as follows. At the first node, $i = 1$, the surface elevation is specified either as an input from the measurements or as some other appropriate function specified at each time step:

$$\zeta_1(t) = f(t) \tag{12}$$

The depth-averaged velocity is computed from the continuity equation for a progressive wave:

$$u_1(t) = \frac{c_1 \zeta_1(t)}{h_1 + \zeta_1(t)} \tag{13}$$

The subscript 1 stands for the quantities at the first boundary node, and c_1 and h_1 denote respectively the phase celerity and water depth at the first node. c_1 is computed from the linear dispersion relation corresponding to Eqs. (5) and (6) for the (dominant) incident wave period.

At the outgoing boundary, $i = n$, we have used the radiation condition both for the surface displacement, when solving the continuity, and for the velocity, when solving the momentum equation:

$$\zeta_t + c\zeta_x = 0 \qquad \text{at } i = n$$
$$u_t + cu_x = 0 \qquad \text{at } i = n$$

(14)

with $c = (gh)^{1/2}$. Eqs. (14) are discretized as follows:

$$\frac{1}{2}\left[\frac{w_{n,j+1} - w_{n,j}}{\Delta t} + \frac{w_{n-1,j+1} - w_{n-1,j}}{\Delta t}\right] = -\frac{c}{2}\left[\frac{w_{n,j+1} - w_{n-1,j+1}}{\Delta x} + \frac{w_{n,j} - w_{n-1,j}}{\Delta x}\right]$$

(15)

where $w = [\zeta, u]^T$.

Condition (14) in principle ensures that the disturbances, with phase velocity c, travel only in the positive x-direction and leave the domain without reflection. On the other hand, waves with phase velocities different from c cannot be expected to radiate away without any problem. For this reason, the above condition is sometimes bolstered with the so-called sponge layer, which damps the outgoing waves either by a viscous or a frictional type — Newtonian cooling — term which has a gradually increasing coefficient within the sponge layer (Israeli and Orszag, 1981).

For obtaining spectral estimates from time domain simulations of random waves it was necessary to perform long runs, which in turn required good absorption of outgoing waves. After trying several sponge-layer-plus-radiation-condition formulations and comparing these results with the radiation-condition-alone computations we have decided to drop the sponge layer because there was no appreciable improvement. Instead, at the expense of some data points, we performed a sequence of cold start computations which enabled us to clean our numerical wave tank before reflected waves could manifest themselves in the domain of interest.

The third spatial derivative of the surface displacement, appearing in Eq. (8), requires some additional effort at the boundary nodes. For the node $i = 2$, at which the computation commences, it is necessary to know ζ_0, the surface displacement just outside the upwave boundary node $i = 1$. Likewise, for the node $i = n - 1$, at which the computation ends, ζ_{n+1}, the surface displacement just outside the last node $i = n$, must be known. We obtain these values by linear extrapolation:

$$\zeta_{0,j} \approx 2\zeta_{1,j} - \zeta_{2,j}$$
$$\zeta_{n+1,j} \approx 2\zeta_{n,j} - \zeta_{n-1,j}$$

(16)

4. Numerical results

4.1. Input data, computational parameters, comparisons

Results of numerical computations, based on the extended Boussinesq model described above, are now compared with experimental results.
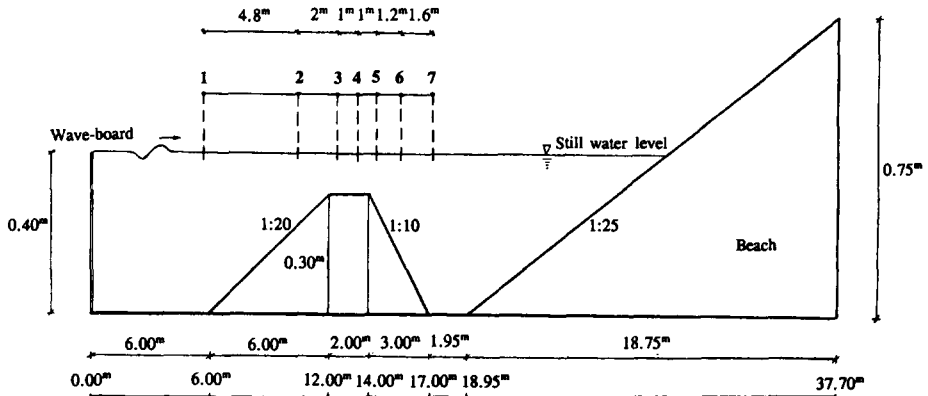
Fig. 1. Longitudinal section of wave flume; the numbers 1 through 7 indicate wave gauge positions.

The experiments were carried out in a wave flume with a submerged trapezoidal bar (see Fig. 1). Free surface displacements were measured by parallel-wire resistance gages at seven stations as shown in Fig. 1. Detailed information about the experiments can be found in Beji and Battjes (1993).

The experiments included breaking and nonbreaking waves. The results shown below are for steep but nonbreaking waves only. These runs were made with periodic incident waves (frequency $f = 0.5$ Hz, wave height $H = 2.0$ cm) as well as random incident waves (JONSWAP-shape spectrum, peak frequency $f_p = 0.5$ Hz, significant wave height $H_s = 1.8$ cm).

Time histories of surface displacement at station 1 and the corresponding depth-averaged velocity were used in the seaward boundary conditions. All cases shown were calculated with Δx approximately equal to $1/70$ of the initial wavelength and Δt equal to $1/50$ of the initial wave period (which corresponded to the 25 Hz sampling rate used in the experiments). Thus, the Courant number, $c(\Delta t/\Delta x)$, at the seaward boundary was nearly one. Spatial and time resolutions of the initial wavelength and period were comparatively high; this was necessary for sufficient representation of the free higher harmonics generated at the lee side of the bar. Indeed for the fourth free harmonic the above resolutions were approximately $1/8$ of the wavelength and $1/12$ of the wave period, respectively. If the computations were to stop before the downslope section, where the free higher harmonics became particularly manifest, less stringent resolutions would be sufficient for obtaining good agreement between computed and measured values.

Fig. 2 shows time domain comparisons of the measured and computed surface displacements for regular waves in the locations of gages 2 through 7. In Fig. 3 time histories of measured surface displacements are compared with the numerical simulations for steep but non-breaking random waves with a JONSWAP type spectrum while corresponding spectral estimates are plotted in Fig. 4, for stations 2–7. The spectral density estimates shown here have 80 degrees of freedom with 15.8% statistical error.

4.2. Discussion of results

Inspection of the figures shows at a glance that the model simulates the observed evolution and decomposition of the wave field very well, for the periodic waves as well as for the
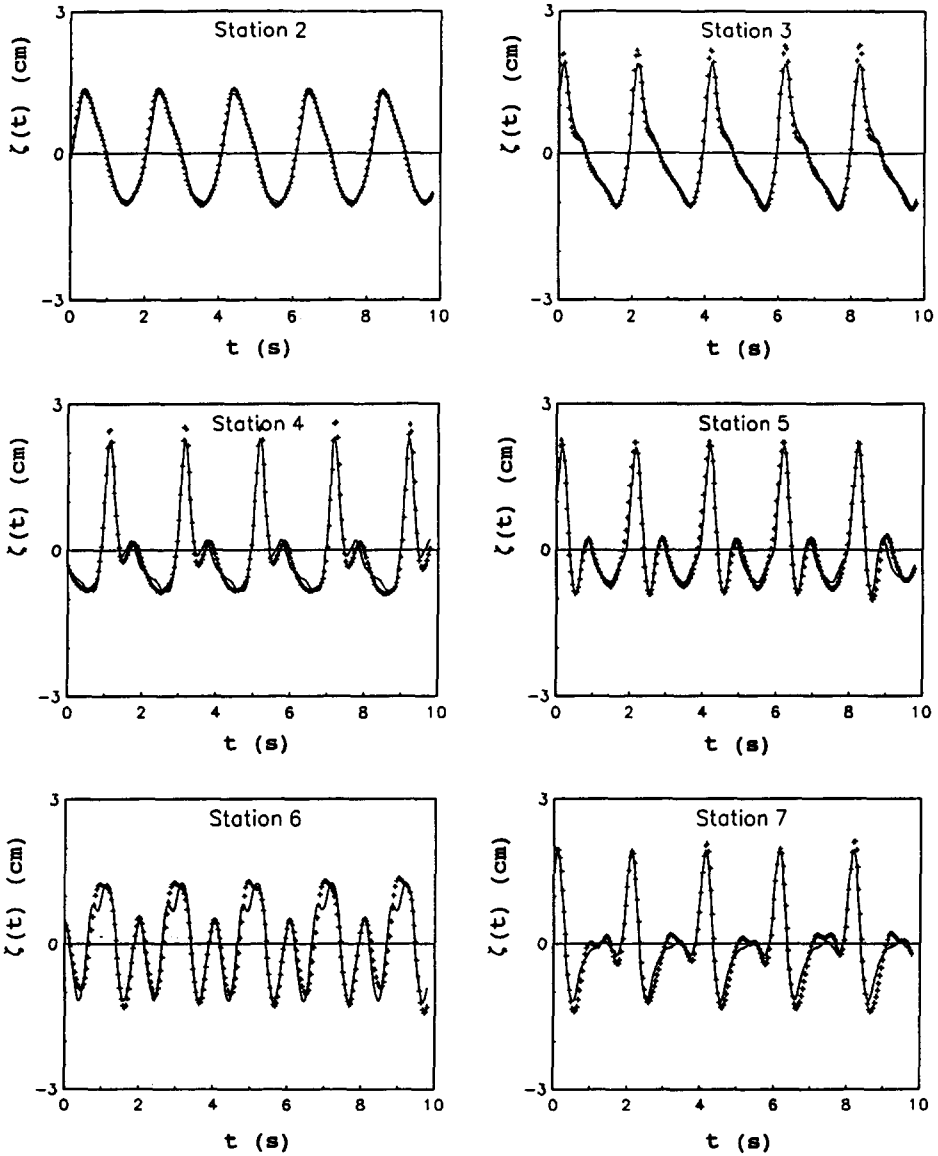
Fig. 2. Surface elevations at several stations for monochromatic incident waves with frequency 0.5 Hz and wave height 2.0 cm. (——) Measured values; (+) values obtained computationally with the improved Boussinesq model.

irregular waves. The initial nonlinear steepening on the seaward slope is well represented, and also the subsequent enhancement of higher harmonics and ensuing profile distortion. The good representation of the wave field even in the area of its decomposition, where free second and higher harmonics propagate in relatively deep water, is particularly noteworthy. This remarkable performance is ascribed to the following points.
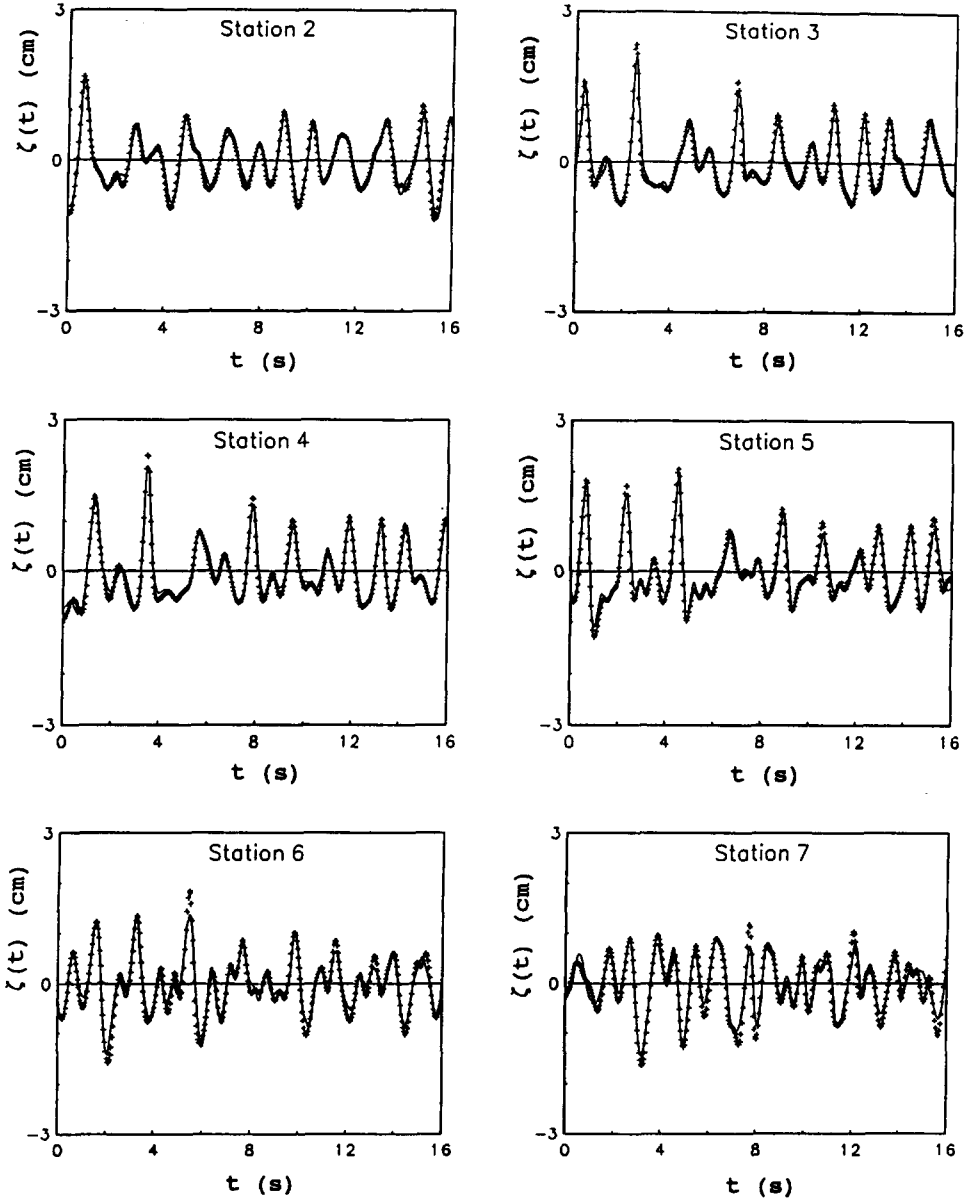
Fig. 3. As in figure 2, except that here the incident waves are random with a JONSWAP-shape spectrum with peak frequency 0.5 Hz and significant wave height 1.8 cm.

First, the improved dispersion characteristics of the Boussinesq model as introduced by Madsen et al. (1991a) allow the propagation of relatively short waves, which is crucial in the downslope region due to the reasons indicated above. Secondly, the refinement introduced into the numerical scheme by the conservative type discretization of the continuity
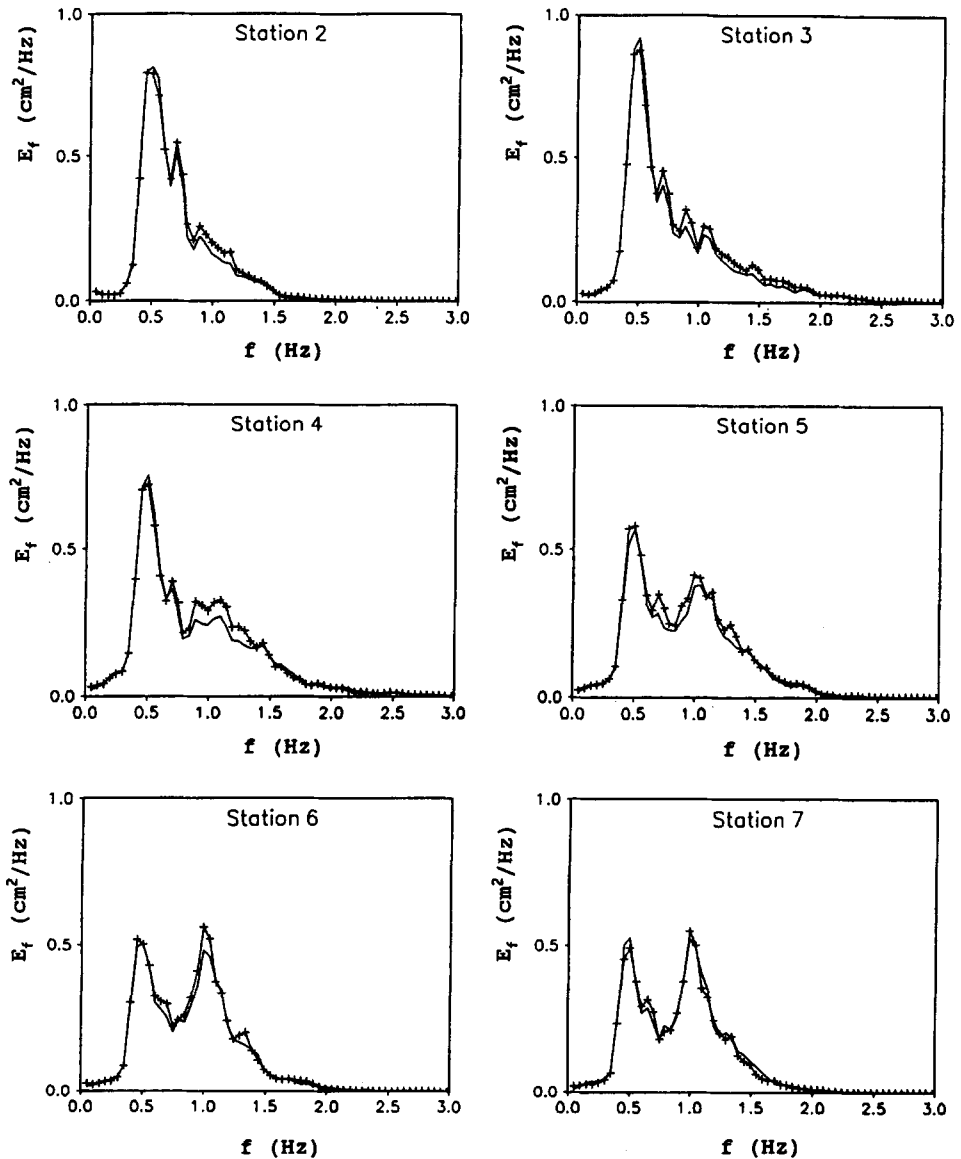
Fig. 4. Spectral density functions of the surface elevations as in Fig. 3; legend as in Fig. 2.

equation instead of the discretization proposed by Peregrine (1967) reduces the total discretization errors and results in better agreements with measurements. Finally, the improved estimation of the nonlinear term provides additional enhancement especially for steep waves.

In order to demonstrate the overall effect of these improvements, results of some computations based on the non-extended Boussinesq equations ($b=0$) and Peregrine's original

numerical scheme are presented. Fig. 5 shows time domain comparisons for regular waves at stations 5, 6, and 7. At station 5 discrepancies between measured and computed values are basically due to the discretization errors of the continuity equation rather than the poor
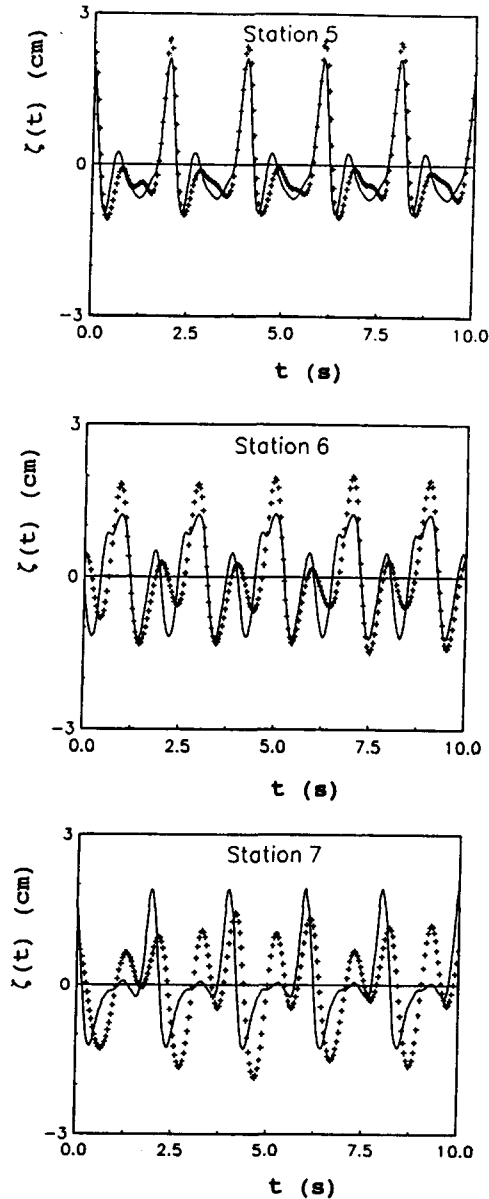

Fig. 5. Surface elevations at stations 5, 6 and 7 for monochromatic incident waves with frequency 0.5 Hz and wave height 2.0 cm. (———) Measured values; (+) values obtained computationally with Peregrine's Boussinesq model.

dispersive characteristics of the original equations because at this station the magnitude of higher harmonics are not yet comparable with the primary wave component. At stations 6 and 7 however the essential cause of the disagreements is the original model's inability to propagate shorter waves. Discretization errors are of secondary importance here.

5. Inclusion of breaking

The experimental results used above are for nonbreaking waves. They are part of a more comprehensive investigation in which also waves were included which were breaking on the bar. The major conclusion of this investigation was that, for the conditions of the experiments, the generation of high frequency energy and its transfer among nearly harmonic wave components due to the nonlinear interactions taking place in the course of the waves' passage over the bar, are hardly affected by wave breaking, which was found to simply re-scale the wave spectrum through overall energy dissipation without changing the spectral shape significantly. A concise substantiation of this statement is offered in Fig. 6, in which
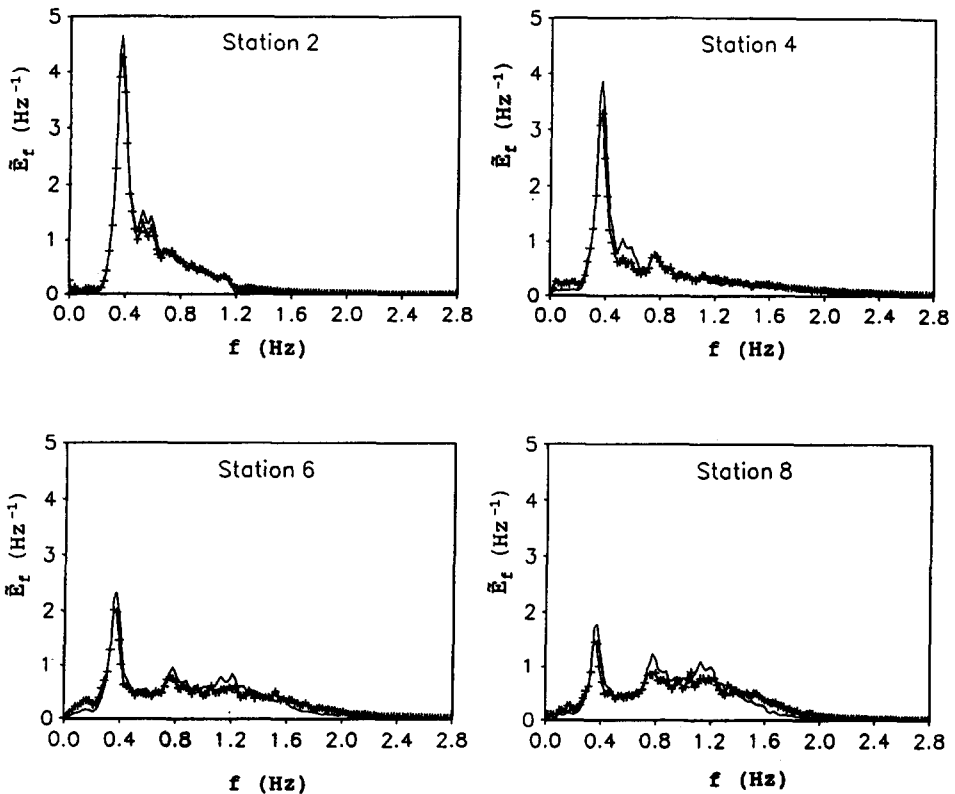

Fig. 6. Normalized measured spectral density functions at four stations for JONSWAP incident spectrum. (———) Nonbreaking waves, (+) plunging breakers.

direct comparisons of normalized spectra for JONSWAP type incident waves, $f_p = 0.4$ Hz, for non-breaking and plunging waves at stations 2, 4, 6, and 8* are made. The normalization is such that the total area under the spectrum for every case is unity. Obviously, the spatial evolutions of the spectral shape follow almost identical trends regardless of the occurrence of breaking.

The aforementioned experimental finding led Battjes and Beji (1991) to suggest a combined model, using the energy-conserving Boussinesq equations for the evolution of the spectral shape, in conjunction with a semi-empirical model to simulate the overall wave energy dissipation due to breaking. Such model has been implemented, using the energy dissipation model of Battjes and Janssen (1978). Preliminary results of this model look very promising (Battjes et al., 1994). A similar combined model has been presented by Mase and Kirby (1992).

6. Conclusions

An improved numerical scheme has been developed for a Boussinesq set of equations with an extension so as to improve the linear dispersion characteristics. The performance of this model has been tested by comparisons with measured surface elevations in waves travelling over a bar. The comparisons, for monochromatic and random waves, clearly demonstrate that the improved Boussinesq equations, as discretized here, are capable of reproducing the essential features and even the details of nonlinear wave transformations over barred topographies, even in the region of rapid wave deformation in deeper water behind the bar. Also, a possible approach is sketched for the inclusion of the effects of wave breaking by combining a semi-empirical energy dissipation formulation, to simulate the overall energy loss, with a Boussinesq-type model for the simulation of the evolution of the spectral shape.

Acknowledgements

Notation

The following symbols are used in this paper:
b calibration factor
c phase velocity;
f wave frequency;
f_p wave frequency at the spectral peak;

---

*These results are from a different set of measurements with eight stations and 0.4 Hz peak frequency.

g gravitational acceleration;
h water depth from still water level;
H wave height;
H_s significant wave height;
i running index for spatial increments;
j running index for time increments;
k wave number, $2\pi/\lambda$;
t time;
u horizontal depth-averaged velocity component;
x horizontal coordinate; and
ζ surface displacement as measured from still water level.

References

Abbott, M.B., 1974. Continuous flows, discontinuous flows and numerical analysis. J. Hydraul. Res., 12(4): 417–467.

Abbott, M.B., Damsgaard, A. and Rodenhuis, G.S., 1973. System 21, ''Jupiter'' (a design system for two-dimensional nearly horizontal flows). J. Hydraul. Res., 11(1): 1–28.

Abbott, M.B., Petersen, H.M. and Skovgaard, O., 1978. On the numerical modelling of short waves in shallow water. J. Hydraul. Res., 16(3): 173–203.

Abbott, M.B., McCowan, A.D. and Warren, I.R., 1984. Accuracy of short-wave numerical models. J. Hydraul. Eng., 110(10): 1287–1301.

Battjes, J.A. and Beji, S., 1991. Spectral evolution in waves traveling over a shoal. In: D.H. Peregrine (Editor), Proc. of the Nonlinear Water Waves Workshop. University of Bristol, Bristol, pp. 11–19.

Battjes, J.A. and Janssen, J.P.F.M., 1978. Energy loss and set-up due to breaking in random waves. In: Proc. 16th Int. Conf. Coastal Eng., Hamburg, pp. 569–587.

Battjes, J.A., Eldeberky, Y. and Won, Y., 1994. Spectral Boussinesq modelling of breaking waves. In: O.T. Magoon (Editor), Proc. Int. Conf. Waves '93, New Orleans, 1993. ASCE, New York, in press.

Beji, S. and Battjes, J.A., 1993. Experimental investigation of wave propagation over a bar. Coastal Eng., 19: 151–162.

Bryant, P.J., 1973. Periodic waves in shallow water. J. Fluid Mech., 59: 625–644.

Byrne, R.J., 1969. Field occurrences of induced multiple gravity waves. J. Geophys. Res., 74(10): 2590–2596.

Dingemans, M.W., 1989. Shift in characteristic wave frequency; some spectra in wave basin and in Haringvliet region. Tech. Rep., Part II, Delft Hydraulics, 56 pp.

Freilich, M.H. and Guza, R.T., 1984. Nonlinear effects on shoaling surface gravity waves. Philos. Trans. R. Soc. Lond., A311: 1–41.

Friedrichs, K.O., 1948. Water waves on a shallow sloping beach. Communs. Pure Appl. Math., 1: 109–134.

Israeli, M. and Orszag, S.A., 1981. Approximation of radiation boundary conditions. J. Comput. Phys., 41: 115–135.

Johnson, J.W., Fuchs, R.A. and Morison, J.R., 1951. The damping action of submerged breakwaters. Trans. Am. Geophys. Union, 32(5): 704–718.

Jolas, P., 1960. Passage de la houle sur un seuil. Houille Blanche, 2: 148–152.

Kirby, J.T., 1990. Modelling shoaling directional wave spectra in shallow water. In: Proc. 22nd Int. Conf. Coastal Eng., Delft, Vol. 1, pp. 109–122.

Madsen, P.A. and Sørensen, O.R., 1992. A new form of the Boussinesq equations with improved linear dispersion characteristics. Part 2: A slowly varying bathymetry. Coastal Eng., 18: 183–204.

Madsen, P.A. and Sørensen, O.R., 1993. Bound waves and triad interactions in shallow water. J. Ocean Eng., 20(4): 359–388.

Madsen, P.A., Murray, R. and Sørensen, O.R., 1991a. A new form of the Boussinesq equations with improved linear dispersion characteristics. Coastal Eng., 15(4): 1–15.

Madsen, P.A., Sørensen, O.R. and Yang, Z., 1991b. Wave–wave interaction in shallow water. In: Proc. XXIV IAHR Congress, Madrid, Vol. B, pp. 3–10.

Mase, H. and Kirby, J.T., 1992. Hybrid frequency-domain KdV equation for random wave transformation. In: Proc. Int. Conf. 23rda Coastal Eng., Venice, Vol. 1, pp. 474–487.

Mei, C.C., 1989. The Applied Dynamics of Ocean Surface Waves. World Scientific, Singapore.

Mei, C.C. and Le Méhauté, B., 1966. Note on the equations of long waves over an uneven bottom. J. Geophys. Res., 71: 393–400.

Peregrine, D.H., 1967. Long waves on a beach. J. Fluid Mech., 27: 815–827.

Prüser, H.H., Schaper, H. and Zielke, W., 1986. Irregular wave transformation in a Boussinesq wave model. In: Proc. 20th Int. Conf. Coastal Eng., Taipeh, pp. 2756–2771.

Rey, V., Belrous, M. and Guazelli E., 1992. Propagation of surface gravity waves over a rectangular submerged bar. J. Fluid Mech., 235: 453–479.

Schaper, H. and Zielke, W., 1984. A numerical solution of Boussinesq type wave equations. In: Proc. 19th Int. Conf. Coastal Eng., Houston, TX, pp. 1057–1072.

Ursell, F., 1953. The long-wave paradox in the theory of gravity waves. Proc. Cambridge Philos. Soc., 49: 685–694.

Witting, J.M., 1984. A unified model for the evolution of nonlinear water waves. J. Comput. Phys., 56: 203–236.

Young, I.R., 1989. Wave transformation over coral reefs. J. Geophys. Res., 94: 9779–9789.